Research highlights: Towards further understanding nanoparticle-cellular membrane interactions

John Pettibone and Stacey Louie*

Materials Measurement Science Division, National Institute of Standards and Technology, Gaithersburg, MD, USA 20899

*Corresponding author: stacey.louie@nist.gov

Nano-impact statement

A better understanding of nanoparticle-cellular interactions is necessary for applied and natural systems, and this knowledge can be gained through multiple approaches, including the development of more accurate model systems, high-throughput assessment screening and manipulation of nanomaterial properties.

Abstract

With the continued increase in commercial and industrial use of nanomaterials, their interactions with biological interfaces in applied and natural systems will need to be understood to improve efficacy and assess ecological risks. Model systems are currently being developed that can be used to evaluate nanomaterial or cellular characteristics affecting the mechanism of attachment and uptake. The development of methods that can provide higher throughput for surveying specific interactions is also valuable for evaluating risk and binning systems of similar behavior, which can direct further detailed examination of specific systems. The first highlighted study demonstrates the development of supported phase segregated lipid bilayers with thoroughly characterized structures, which were subsequently used for evaluating specific chemical and morphological properties contributing to observed nanoparticle-membrane interactions. The second study employs a high throughput approach for evaluating lipid bilayer-nanoparticle interactions by using arrays of bilayers on a chip. The arrays provide a large parameter space to be examined, which included changes in both solution and membrane composition. The last study demonstrates the importance of the nanoparticles' mechanical properties on uptake by the cellular membrane using a combined experimental and computational approach.

The interaction of nanomaterials with eukaryotic cells in environmental systems can involve complex processes resulting in distinct biological responses, which can include penetration and endocytotic uptake (Neal, *Ecotoxicology*, 2008, **17**, 362). Furthermore, cellular membranes are composed of domains with unique compositions of phospholipids that contain distinct shapes, sizes, charge, and functionality (Semrau and Schmidt, *Soft Matter*, 2009, **5**, 3174). Thus, the composition controls local packing, structure and mobility, and the interaction of the organism with nanomaterials will be dependent on these local heterogeneities. Nanomaterial physicochemical properties also strongly influence this interaction (Verma and Stellacci, *Small*, 2010, **6**, 12). The mechanistic understanding of these interactions can be improved by developing model systems that better replicate biological structures and providing more thorough characterization of either the nanoparticle or membrane or both. Furthermore, direct measurements of these interactions on model systems will provide more insight into the mechanisms occurring in natural systems.

Probing the nano-bio interface through supported membrane-nanoparticle interactions

The work by Melby et al. (Melby et al., *Environ. Sci: Nano*, 2015) describes the development of model membranes on silica substrates to examine specific interactions of nanoparticle attachment to different phase segregated domains, using unilamellar vesicles comprising different mole fractions of 1,2-dioleoyl-sn-glycero-3-phosphocholine (DOPC), octadecanoyl (SM), and cholesterol (Chol) at low concentrations relative to previously reported studies. The authors highlight the importance of introducing a lower vesicle concentration (0.03 mg mL^{-1}) of the unilamellar structures to the substrates that allow the vesicles to rupture and subsequently form the supported lipid bilayer. When the concentration of the primary structures is too high, the vesicles can adsorb to the bilayer. The compositions of the bilayers that were examined along with predicted phase boundaries are shown in the ternary phase diagram in Figure 1 (left image).

A suite of instruments was used to investigate the bilayer structures forming from different lipid mixtures, including quartz crystal microbalance with dissipation monitoring (QCM-D), atomic force microscopy (AFM), and super-resolution fluorescence structured illumination microscopy (SIM). QCM-D experiments used a silica crystal to measure changes in resonance frequency that are related to mass, and the energy dissipation, which provides information regarding the interaction of the analyte and substrate. First, the optimized composition of DOPC, SM, and Chol at 0.6/0.2/0.2 mole fractions were examined and compared to DOPC alone, which is expected to create a liquid disorder phase, L_d, only. The change in the resonance frequency for the DOPC membrane alone after stabilization was lower than for the DOPC/SM/Chol bilayer, which indicates higher mass for the three component system resulting from an increased packing density. AFM was used to examine the topography of the bilayers, and changes in height were near 1 nm, which were described as distinct phases in the bilayer of the mixed lipid system. Furthermore, no adsorbed unilamellar vesicles, which had measured hydrodynamic diameters greater than 70 nm, were detected with AFM.

The incorporation of different fluorescently labeled lipids into the vesicles that are associated with either the L_d or liquid ordered domains, L_o, allowed utilization of SIM to examine the morphology of the supported bilayer structures with sub-100 nm resolution. Demonstration of the fluorescence mapping of the lipid bilayers is presented in Figure 1 (right image labeled A-C). Implementing multiple tags

associated with the L_d phase resulted in images with dark regions not associated with DOPC. To examine the dark regions, ganglioside G_{M1} was incorporated, which associates with the L_o phase and can be tagged by another fluorescent label, and demonstrated that the dark regions indeed consisted of SM and Chol. The procedure resulted in phase segregated domains that could be used as a model system for studying membrane-nanomaterial interactions.

To examine the interactions of the model phase segregated membranes with nanoparticles, cationic (amine) and anionic (carboxyl) functionalized 4 nm Au particles were examined in different ionic strength media. The cationic nanoparticles showed irreversible attachment to the negatively charged bilayers. The observed frequency changes in QCM-D experiments indicated that the extent of attachment increased for all bilayers in lower ionic strength media, which was attributed to the more negative zeta potential, ζ, of the bilayer and decreased degree of observed nanoparticle aggregation. However, differences in initial rates of attachment were observed for pure DOPC and mixed lipid bilayers in higher ionic strength media, even though ζ was nearly identical. The authors concluded that the morphology of the bilayers contributed significantly to the interaction. Further evidence for the contribution of the bilayer morphology was also observed when ζ became more negative upon incorporation of G_{M1} but resulted in no significant difference in attachment. The attachment of the anionic nanoparticles was below the limit of detection, which the authors attributed to Coulombic repulsion. Overall, the work demonstrates the formation of phase-segregated lipid bilayers that can be used as model systems to begin studying the factors that contribute to membrane-nanoparticle interactions in environmental systems. Further work in understanding the interaction between the substrate and bilayers, which can be probed further with dissipation measurements, is also an active research area.
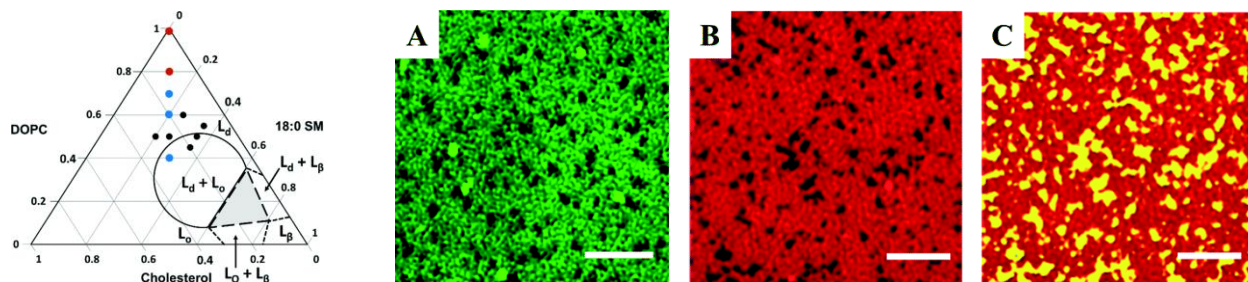

Figure 1. (left image) Ternary phase diagram showing the composition of vesicles from which supported lipid bilayers were successfully formed on SiO_2 substrates as monitored by QCM-D. (right images) A-C SIM microscopy images displaying the spatial distribution of fluorescently-labeled phospholipids, which differentiate L_o and L_d domains in supported lipid bilayers. Scale bars are 2 μm. Reprinted with permission from Melby et al., *Environ. Sci. Nano*, 2015. Copyright 2015 Royal Society of Chemistry.

Assessing cellular-nanoparticle interactions in bilayer lipid arrays

Because of the increasing probability of nanoparticle exposure to eukaryotic organisms, the development of tools for higher throughput assessment to survey differences in interaction and risk is ideal. Here, current research demonstrates the implementation of bilayer lipid arrays to examine the interaction of cationic and anionic polymeric nanoparticles in different media.

The work by Lu et al. (Lu et al., *Nanoscale*, 2015, **7**, 7858) describes the investigation of polystyrene nanoparticles terminated with amine or carboxyl functionality that were exposed to a broad distribution of bilayer lipid compositions and media components. Previous work by the researchers (Lu et al., *Biotechnology Journal*, 2014, **9**, 446) demonstrated the development of a 32-element array to form

bilayers that could measure rupture, characterize the formation and presence of pores, and determine relative rates of these processes induced by the presence of nanoparticles (Figure 2). First, the authors examined the stability (which was defined by rupture) of lipid bilayers comprising 1-palmitoyl-2-oleoyl-*sn*-glycero-3-phos-phocholine (POPC), 1-palmitoyl-2-oleoyl-*sn*-glycero-3-phosphoethanolamine (POPE), Chol, 1-palmitoyl-2-oleoyl-*sn*-glycero-3-phospho-L-serine (POPS), and Cerebroside (CB) in different mole fractions in the presence of the cationic and anionic nanoparticles at different concentrations. Overall, similar results to the previously described study (*vide supra*) and others [see references within the article by Lu et al. (Lu et al., *Nanoscale*, 2015, **7**, 7858)] demonstrated rupturing for all negatively charged membranes with the cationic nanoparticles, but no statistical difference in membrane rupturing was observed for the anionic nanoparticles.

Ionic strength and pH dependence were observed for the interaction between the membrane and cationic nanoparticles, which the authors attributed to charge screening and osmotic pressure contributions that limit interaction in the case of increasing pH. The rate of observable ruptures in the different bilayer mixtures also was retarded at higher pH. When the membrane charge was neutral, interaction with the cationic nanoparticles was still observed, but minimal interaction was detected with positively charged membranes. In contrast, no interaction with the positive, neutral or negative membranes was observed for the anionic nanoparticles, which was suggestive of other factors contributing to the membrane-nanoparticle interaction other than electrostatic forces (*e.g.*, nanoparticle size, membrane structure, etc.).

The nanoparticle-bilayer interaction resulted in the formation of pores that could be monitored and modeled on the array. Pore sizes were modeled as electrolyte filled cylinders with lengths similar to the bilayer thickness – 5 nm. Both transient and persistent pore formation was reported by the authors, which were not sensitive to applied voltage in the (20 to 70) mV range, and resulted in current measurements that were consistent with (0.3 to 2.6) nm pore radii. Further results for the cationic nanoparticles showed the appearance of pores was greater for negatively charged films compared to neutral films, which the authors attributed to larger pores due to increased bilayer-nanoparticle interaction or increased conductivity at the surface due to high cation concentration associated with the negative bilayers. Increased numbers of pores were observed at positive applied voltages, which the authors describe as evidence for increased probability of pores in the presence of higher concentrations of cationic nanoparticles.

Exposure of the cationic nanoparticles to fetal bovine serum resulted in almost complete elimination of detectable interactions between the membrane and aged particles, which suggest that an understanding of aging in biological or environmental systems is also critical to predict cellular response. Overall, the work describes a chip-based method to provide high throughput assessment of nanoparticles with a broad range of lipid bilayer mixtures, which should prove valuable when combined with more detailed mechanistic studies.
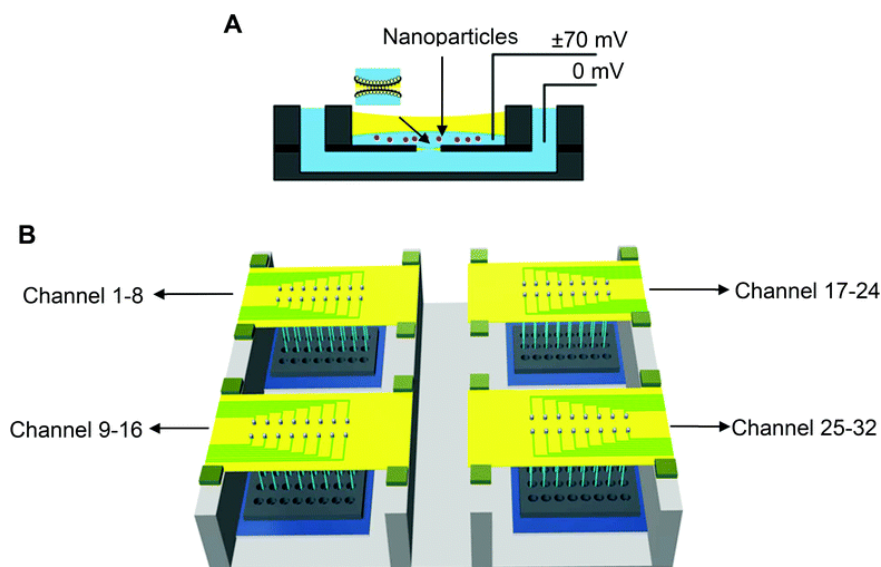
Figure 2. (A) To form bilayers, lipid-containing aqueous solution is first added to the bottom channel through the outer wells. Oil is then added to the central well for lipid monolayer formation at the aqueous/oil interface, constrained by a masking aperture. Aqueous solution is added to the central well to form another lipid monolayer. Bilayer formation begins (inset) after introducing additional aqueous solution through the outer well. Nanoparticles were added to the central well after bilayer formation. (B) Apparatus schematic for simultaneous bilayer formation and measurement in 32 wells. Reprinted with permission from Lu et al., *Nanoscale*, 2015, *7*, 7858. Copyright 2015 Royal Society of Chemistry.

Controlling cell-nanoparticle interaction through mechanical properties

Understanding how to control the interaction of nanomaterials with cells will increase the efficacy of engineered materials in applied systems and predictability in natural systems. The development of methods for examining the contributions of the cellular membrane characteristics, as outlined in the previous studies (*vide supra*), as well as methods for functionalizing the nanoparticle surface are two different approaches to improve the understanding and exploitation of the nano-bio interface.

In the work by Zhang et al. (Zhang et al., *ACS Nano*, 2015, *9*, 9912) the role of polymeric nanoparticle surfaces functionalized with different lipid structures and their contribution to cellular uptake were examined. More specifically, methods for varying the lipid shell structure on the nanoparticle surface were developed, and the role of the distinct lipid structure on the interactions of the nanoparticles with the cells was examined experimentally and computationally. The authors previously demonstrated correlation between nanoparticle rigidity and cellular uptake controlled by interfacial water between the core and the lipid shell (Sun et al., *Adv. Mater.*, 2015, *27*, 1402). To further examine the role of the nanoparticle rigidity on uptake, the authors controlled the lipid shell structure in the current study. First, the development of synthetic methods to control the lipid coverage thickness (monolayer versus bilayer structure) on a poly(lactide-*co*-glycolide) (PLGA) core was achieved using a two-stage microfluidic chip. The structure of the lipid layer on the nanoparticles was controlled based on the method for generation, which included either precipitation of the core followed by introduction of a lipid solution (monolayer formation, MP) or introduction of liposomes followed by addition of nanoparticle cores under controlled mixing for rearrangement of liposomes on the nanoparticle surface (bilayer formation, BP). Characterization of the size distribution of the two distinct products was conducted with a suite of instrumentation.

Cryogenic transmission electron microscopy (cryo-TEM) was used to determine the thickness of the bilayer structure, which was found to be approximately 4 nm and was able to be differentiated due to the presence of interfacial water and weak interaction with the core surface. No differentiation of the lipid and the core was identified of the monolayer structure, which the authors attributed to the weak contrast and interaction of the hydrophobic tails of the lipid with the nanoparticle surface. The increase in the average hydrodynamic diameter of the nanoparticles (measured by dynamic light scattering) upon formation of the MP and BP structures was consistent with the cryo-TEM results. Next, fluorescence quenching experiments were used to determine the relative lipid concentrations on the nanoparticles. The relative amounts of quenching agent necessary to reduce the fluorescence of the tagged NPs to background intensities were consistent with monolayer and bilayer structures.

To test the mechanical properties of the MP and BP structures, AFM was used along with molecular dynamics (MD) simulations. The AFM results showed the BP structures to display higher deformation and energy dissipation than the MP structures. The large deformation of the BP structure was attributed to the high flexibility of the lipid shells, which have previously been described as fluidic and elastic. Further evidence for flexibility was observed in the larger energy dissipation measured with BP structures, which the authors attributed to a larger contact area at the tip-nanoparticle interaction that results in greater frictional forces. MD simulations corroborated the mechanism of increasing dissipation energy due to deformation of the BP layer that was not observed in the MP systems; thus, providing further evidence for the flexibility of the BP structure on the synthesized hybrid nanoparticles.

After the thorough physicochemical characterization of the hybrid products, their efficacy as drug delivery vehicles was examined *in vitro*. Using confocal fluorescent microscopy, the cytotoxicity of the drug-loaded MP and BP was higher for the MP structures compared to the BP structures and the free drug alone. The authors attributed the decreased uptake efficiency of the BP structures to an increased difficulty to internalize the nanoparticles due to the high dissipation energies at the cell-particle interface described previously. Furthermore, the authors stated that the uptake mechanism was the same for both particles, but is inconsistent with micron size species and suggested size dependent effects should be further explored. Overall, the study provides further insight into the contributions of the nanoparticle-cell interaction that could be exploited in other applied systems.
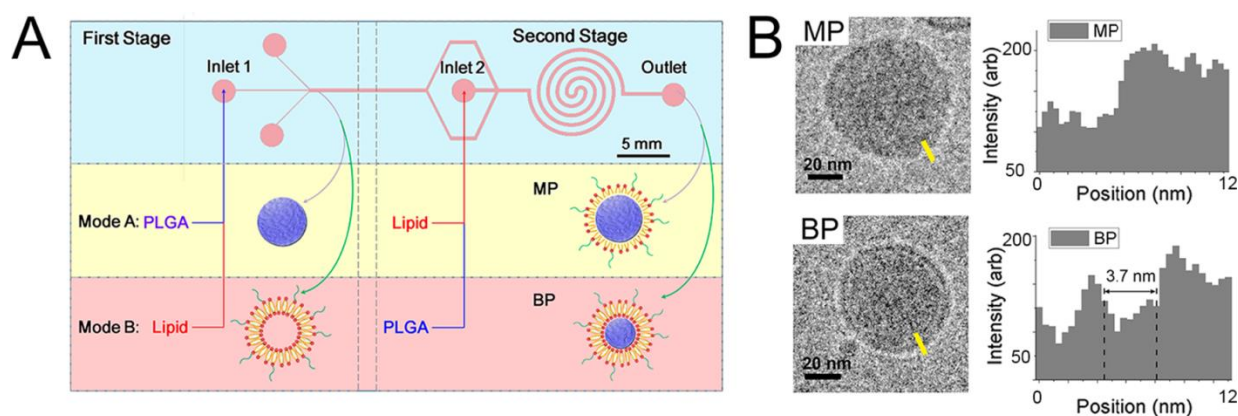

Figure 3. A) Schematic of the two-stage microfluidic chip and characterization of hybrid nanoparticles with varying lipid shells.

(B) Cryo-TEM images of MPs and BPs. The electron density across the lipid layer structure (indicated by the short yellow line) shows the lipid bilayer structure of BPs, which is 3.7 nm thick. Reprinted with permission from Zhang et al., *ACS Nano*, 2015, *9*, 9912. Copyright 2015 American Chemical Society.